npg

ORIGINAL ARTICLE

Mouse mesenchymal stem cells inhibit high endothelial cell activation and lymphocyte homing to lymph nodes by releasing TIMP-1

L Zanotti[1,12,13], R Angioni[2,3,13], B Calì[2,3], C Soldani[1], C Ploia[1], F Moalli[4], M Gargesha[5], G D'Amico[6], S Elliman[7], G Tedeschi[8,9], E Maffioli[9], A Negri[8,9], S Zacchigna[10], A Sarukhan[11], JV Stein[4] and A Viola[2,3]

Mesenchymal stem cells (MSC) represent a promising therapeutic approach in many diseases in view of their potent immunomodulatory properties, which are only partially understood. Here, we show that the endothelium is a specific and key target of MSC during immunity and inflammation. In mice, MSC inhibit activation and proliferation of endothelial cells in remote inflamed lymph nodes (LNs), affect elongation and arborization of high endothelial venules (HEVs) and inhibit T-cell homing. The proteomic analysis of the MSC secretome identified the tissue inhibitor of metalloproteinase-1 (TIMP-1) as a potential effector molecule responsible for the anti-angiogenic properties of MSC. Both *in vitro* and *in vivo*, TIMP-1 activity is responsible for the anti-angiogenic effects of MSC, and increasing TIMP-1 concentrations delivered by an Adeno Associated Virus (AAV) vector recapitulates the effects of MSC transplantation on draining LNs. Thus, this study discovers a new and highly efficient general mechanism through which MSC tune down immunity and inflammation, identifies TIMP-1 as a novel biomarker of MSC-based therapy and opens the gate to new therapeutic approaches of inflammatory diseases.

INTRODUCTION

Mesenchymal stem cells (MSC) are multipotent progenitor cells with self-renewable capacity and the potential to differentiate into various mesodermal lineages.[1] MSC are present in the stromal fraction of many tissues, where they reside close to blood vessels,[2] a trait that is shared with pericytes. Indeed, when analyzed *in vitro*, MSC and pericytes display similar morphological and functional features, although the two cell types are likely to have different functions *in vivo*.[3] Although pericytes regulate capillary homeostasis and architecture,[4] the *in vivo* functional role of MSC is less clear and it is likely to be tissue-specific. For example, in the bone marrow, MSC contribute to the formation of the 'niche' for the hematopoietic stem cells (HSC), thus providing an appropriate microenvironment for hematopoiesis.[5] In other tissues, MSC may be involved in homeostatic control and tissue repair.[6]

A well-established feature of MSC is their ability to inhibit inflammation and immunity, both *in vitro* and *in vivo*. In mouse models of human diseases, MSC have been shown to be highly immunosuppressive being effective, for example, in the treatment of experimental autoimmune encephalomyelitis,[7] collagen-induced arthritis[8] or graft-versus-host disease.[9] On the basis of these experimental results, MSC are now used in several clinical trials (see www.clinical trials.gov) and represent a new frontier in cellular therapy. The anti-inflammatory effect of MSC can be largely explained by their ability to secrete a vast array of soluble mediators with immunomodulatory properties, such as interleukin-10 (IL-10), prostaglandin E2, transforming growth factor, nitric oxide (for mouse MSC) and indoleamine-2,3-dioxygenase (for human MSC), and tumor necrosis factor-α (TNF-α)-stimulated protein 6 (ref. 9–11) that may act in a paracrine or endocrine manner. However, a unifying mechanism of action is still missing, and it is likely that other specific mediators and targets explaining the *in vivo* immunosuppressive effects of MSC remain to be identified.

Both inflammatory and immune responses depend on migration of leukocytes. Recruitment of neutrophils and monocytes into inflamed tissues is directed by chemokines induced by inflammatory stimuli, including bacterial lipopolysaccharide, IL-1 and TNF-α.[12,13] On the other hand, adaptive immunity starts in secondary lymphoid organs, where naive antigen-specific T cells encounter dendritic cells loaded with cognate antigen. For this to occur, T cells must enter lymph nodes (LNs) via specialized post-capillary venules that are made up of endothelial cells with cuboidal morphology and therefore called high endothelial venules (HEVs).[14,15] Endothelial cells have a major role in these processes, changing their phenotypes to support various phases of the inflammatory responses. The capacity of leukocytes to interact with the endothelium is determined by the activation of

[1]Humanitas Clinical and Research Institute, IRCCS, Rozzano, Milan, Italy; [2]Department of Biomedical Sciences, Venetian Institute of Molecular Medicine (VIMM), Padua, Italy; [3]University of Padua, Italy, Switzerland; [4]Theodor Kocher Institute, University of Bern, Bern, Switzerland; [5]BioInVision Inc., Cleveland, OH, USA; [6]Centro Ricerca 'M. Tettamanti,' Clinica Pediatrica Università degli Studi di Milano Bicocca, Monza, Italy; [7]Orbsen Therapeutics Ltd, National University of Ireland, Galway, Ireland; [8]Department of Veterinary Science and Public Health, University of Milano, Milano, Italy; [9]Filarete Foundation, Milano, Italy; [10]International Centre for Genetic Engineering and Biotechnology (ICGEB), Padriciano, Trieste, Italy and [11]INSERM, Paris, France. Correspondence: Dr L Zanotti, Division of Regenerative Medicine, Stem Cells and Gene Therapy, San Raffaele Hospital, via Olgettina 48, Milan 20100, Italy.
E-mail: zanotti.lucia@hsr.it
[12]Current address: Division of Regenerative Medicine, Stem Cells and Gene Therapy, San Raffaele Hospital, Milan, Italy.
[13]These authors contributed equally to this work.

endothelial cells that in turn leads to the expression of a variety of chemoattractants and surface adhesion molecules including intercellular adhesion molecule-1 (ICAM-1) and vascular cell adhesion molecule-1 (VCAM-1).[16] In addition, if the inflammatory stimulus persists, then angiogenesis is initiated by the migration of endothelial cells lining the venules into the tissue.[16,17] The generation of new blood vessels is required for the survival of inflammatory cells within the tissue, and thus inhibition of factors that promote angiogenesis may reduce inflammation and prevent its pathological consequences such as inflammatory tissue damage, autoimmunity, fibrosis or tumor growth.[16,18]

In this study, we have identified the endothelium as a specific and novel target of MSC-based therapy.

MATERIALS AND METHODS

Mice
C57BL/6J mice were purchased from Charles River Laboratories (Calco, Italy). All mice used as primary cell donors or recipients were between 8 and 12 weeks of age. Procedures involving animals and their care conformed to institutional guidelines in compliance with national (4D.L. N.116, G.U., suppl. 40, 18-2-1992) and international (EEC Council Directive 2010/63/UE; National Institutes of Health Guide for the Care and Use of Laboratory Animals) law and policies. The protocol was approved by the Italian Ministry of Health on 18 June 2007 and modified by Protocol 162/2011-B. All efforts were made to minimize the number of animals used and their suffering. In all the experiment, the mice were sex and age matched, no further randomization was applied.

Isolation of murine MSC
Detailed protocols are available in the Supplementary Materials and Methods.

Collection of conditioned medium
Detailed protocols are available in the Supplementary Materials and Methods.

Endothelial cell lines
Detailed protocols are available in the Supplementary Materials and Methods.

In vitro endothelial cell activation
Detailed protocols are available in the Supplementary Materials and Methods.

Tube formation assay
Detailed protocols are available in the Supplementary Materials and Methods.

Immunization with Complete Freund Adjuvant/Ovalbumin
In all, 1 mg/ml Ovalbumin (OVA) (Sigma-Aldrich, Steinheim, Germany) was emulsified in Complete Freund Adjuvant (CFA) (Sigma-Aldrich), and 100 μl of emulsion was injected subcutaneously (s.c.) in three sites in the back. After 24 h, 1×10^6 MSC were injected s.c. in the lumbar region. Immunized mice were killed 4 days later, and the brachial draining LNs (dLNs) were collected and frozen in OCT for immunofluorescence or digested for FACS analysis.

In vivo tissue inhibitor of metalloproteinase-1 immunoneutralization
Goat polyclonal anti-TIMP-1 IgG[19] (catalog no. AF980; R&D Systems, Minneapolis, MN, USA) was intravenously (i.v.) administered (0.5 mg/kg) in immunized mice 18 h after MSC transplantation. As a control, additional mice were given equivalent doses of an isotype-matched goat IgG (catalog no. AB-108-C, R&D Systems). Immunized mice were killed 2 days later, and the brachial dLNs were collected and digested for endothelial cell analysis

by FACS. Data are representative of 36 LNs/group analyzed from four independent experiments.

Tissue inhibitor of metalloproteinase-1 siRNA reverse transfection
Timp-1 Silencer Select Pre-designed siRNAs (Ambion, Waltham, MA, USA) were exploited for mMSC transfection, and Silencer Select Negative Control No. 1 siRNA (Ambion) was adopted as scramble. siRNAs were diluted in Opti-MEM I reduced Serum Medium (Gibco, Waltham, MA, USA) at the final concentration of 50 nM. Diluted siRNAs were placed 100 μl/well in a 24-well tissue culture plate in the presence of 1 μl of Lipofectamine-2000 (Invitrogen, Carlsbad, CA, USA), according to the manufacturer's instructions. Murine MSC were seeded at a density of 6×10^4 cells/well and cultured in antibiotic-free medium. Medium was replaced 24 h post transfection with fresh DMEM low Glucose, 2 mM L-glutamine and 10% FCS Biosera. mMSC tissue inhibitor of metalloproteinase-1 (TIMP-1) secretion was analyzed at 24, 48 and 72 h after transfection by ELISA (R&D Systems). In vivo data with siRNA MSC are representative of 20 dLNs from 2 independent experiments.

AAV-mediated TIMP-1 overexpression
All the AAV vectors used in this study were generated by the AAV Vector Unit (AVU) at ICGEB Trieste (http://www.icgeb.org/avu-core-facility.html) as described previously.[20] Briefly, AAV vectors of serotype 9 were produced in HEK293T cells, using a triple plasmid co-transfection method. Viral stocks were collected after CsCl$_2$ gradient centrifugation. The total number of viral genome was determined by real-time PCR; the viral preparations had titers between 1×10^{13} and 3×10^{13} viral genome (vg) particles per ml. AAV9-TIMP-1 was intraperitoneally injected at a dose of 2×10^{11} vg in 100 μl PBS −/−. Equal amount of AAV9-LacZ was used as a control. One day after AAV9 administration, mice were immunized with CFA/OVA as discussed above (6 mice/group). Brachial dLNs were collected 4 days after immunization and digested for FACS analysis. Data are representative of one experiment out of two.

Immunofluorescence
Detailed protocols are available in the Supplementary Materials and Methods.

Flow-cytometry analyses
Detailed protocols are available in the Supplementary Materials and Methods.

LC-ESI MS/MS analysis
Detailed protocols are available in the Supplementary Materials and Methods.

Optical projection tomography
In all, 5 μg of Alexa-594 MECA-79 antibody (conjugated according to the manufacturer's instructions using the Alexa-594 conjugation kit; Invitrogen) was injected i.v. 15 min before organ harvest. Brachial LNs were excised, cleaned of surrounding fat and then incubated with AlexaFluor 488-conjugated anti-B220 (0.67 μg/ml) as previously described.[21] Further details are described in the Supplementary methods.

3D immunofluorescence
Mice were immunized and transplanted as described above. On day 3 after immunization, single-cell suspensions were obtained from LNs of C57/Bl6 wt mice. CD4+ T cells were isolated using the mouse CD4+ T cell isolation kit (Stem Cell Technologies, Vancouver, BC, Canada), according to the manufacturer's protocol. The lymphocytes were fluorescently labelled, injected i.v. into CFA/OVA immunized recipient mice and allowed to home for 20 min before blocking further homing with anti-L-selectin mAb. After 20 min, dLNs were isolated, treated and analyzed as previously described.[22] Data are representative of eight (CFA/OVA) and nine (+MSC) mice from three independent experiments.

Cryo imaging
MSC labelled with qTracker 655 (Life Technologies, Oslo, Norway) were s.c. injected into a control mouse or a mouse previously immunized with CFA/

OVA. Mice were killed 4 days later, frozen and cryo-imaged using the CryoViz cryo-imaging system (BioInVision, Inc., Cleveland, OH, USA) as described in Roy et al.[23,24] Cryo-images were acquired using the ProSCI software as described in Roy et al.[24] Further details are described in the Supplementary methods.

Statistical analysis

The sample size per group was estimated from previous experience with similar experiments. There were no pre-established criteria for mice or sample exclusion: except evident technical damage. Data were collected and analysis was done without the investigator knowing group allocation. Data were analyzed using the Prism Software (GraphPad, La Jolla, CA, USA). Data were expressed as mean ± s.e. Differences were assessed using t-test, Mann–Whitney test or one-way ANOVA. Statistic tests were performed between data with similar variance. Results with a P-value of < 0.05 were considered as significant.

RESULTS

MSC transplantation affects endothelial activation in immune reactive LNs

We have previously shown that encapsulated MSC injected s.c. are able to control systemic and local inflammation through the release of soluble factors.[9] Moreover, we have demonstrated that subcutaneous administration of MSC is more efficient than the intravenous route, probably because most of the MSC injected i.v. are trapped in the lungs and cleared after a few days.[9,25–27] On the basis of our previous data indicating that encapsulation was not required to improve the efficacy of s.c. injected MSC,[9] in this study we performed subcutaneous injections of free MSC (not encapsulated) in the lumbar area of mice that had been previously immunized with OVA in CFA (CFA/OVA) in the upper dorsal region. As expected, the immunization induced a robust and rapid response in the brachial dLNs (Figure 1). MSC transplantation significantly reduced this response, decreasing both the total cellularity and the volume of dLNs and affecting the recruitment of specific cell populations (Figures 1b–e), as already described.[9] Using whole-mouse cryo-imaging analysis,[28] we verified that s.c. injected MSC did not migrate away from the site of injection during the experimental time (5 days), both in immunized and in untreated mice (Supplementary Movies S1 and S2). Together with

our previous study,[9] these data indicate that MSC are able to dampen inflammation through the release of soluble mediators.

LN growth during immune responses is accompanied by endothelial activation and vascular expansion, two events that are required for leukocytes recruitment and orchestration of immunity. We analyzed the expression of two adhesion molecules, VCAM-1 and ICAM-1, that are typically upregulated on the inflamed endothelium (Figures 2a–d). Interestingly, the dLN vessels of mice treated with MSC had a lower expression of both VCAM-1 and ICAM-1, as demonstrated by the colocalization analysis expressed as Mander's coefficient (Figures 2b–d). Moreover, we observed that the dLNs of mice transplanted with MSC showed reduced density of the endothelial marker CD31 and of Lyve-1, a marker of the lymphatic endothelium, suggesting a reduced vascular expansion upon MSC treatment (Figures 2a, c and e).

Altogether, these data indicate that MSC inhibit activation of vascular and lymphatic endothelium in the dLNs of immunized mice.

MSC inhibit activation and elongation of HEVs and affect recruitment of T cells to dLNs

The migration of leukocytes from the blood stream into LNs occurs via HEVs, which are post-capillary venules structurally adapted to support lymphocyte trafficking. Because of the reduced numbers of leukocytes present in the dLNs of mice treated with MSC (Figure 1),[9] we asked whether MSC transplantation affects HEV activation, lymph-node vascularization and leukocyte migration in vivo.

MSC were s.c. injected in the lumbar region of mice that had been previously immunized in the dorsal region with CFA/OVA, as already described (Figure 1), and HEV cells in brachial LNs were analyzed. In particular, HEV cells were identified as CD45⁻CD31⁺ PNAd⁺ cells (Supplementary Figure S1). The reduced number of CD45⁻CD31⁺ cells was confirmed by flow-cytometry analyses (Figure 3a) and can be explained by the inhibition of endothelial cell proliferation in MSC-treated mice, as shown by the reduced uptake of BrdU (Figure 3b). In the dLNs of mice treated with MSC, we observed a reduction in the absolute number of HEV cells as compared with controls (Figure 3c). Moreover, HEV cells had a reduced expression of VCAM-1 (Figure 3d).
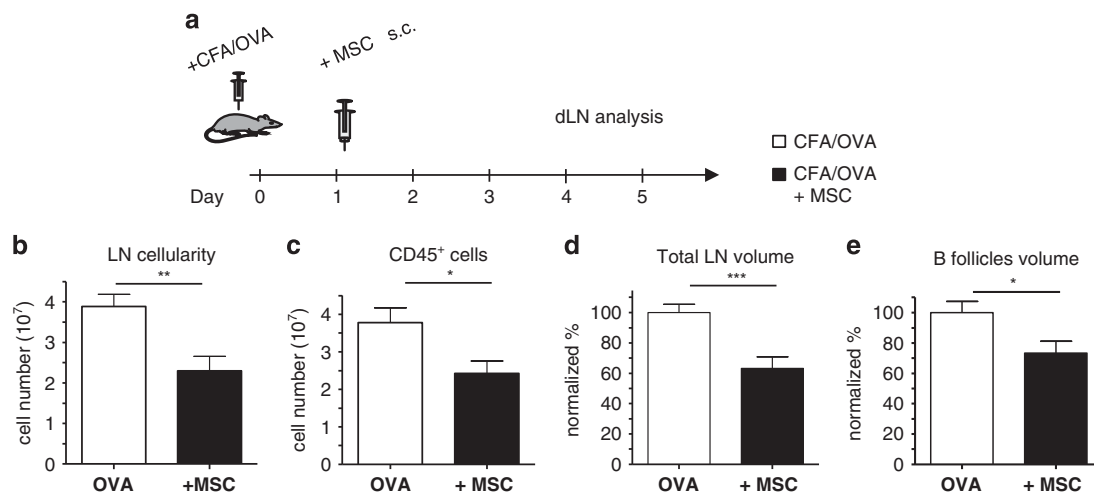

Figure 1. MSC affect size and cellularity of dLNs. (**a**) Diagram of the experimental protocol designed to investigate the influence of MSC transplantation. Mice were immunized in the dorsal back with CFA/OVA on day 0 and, on day 1, a group of animals received subcutaneous injection of 10^6 MSC in the lumbar back. On days 4–5, depending on the subsequent analyses, brachial LNs were collected and processed. (**b**, **c**) On day 5, dLNs were digested and analyzed by flow cytometry. Data are representative of eight mice from two independent experiments; (**d**, **e**) OPT data are expressed as percentage on OVA average. In (**b–e**), error bars represent s.e. (*P < 0.05; **P < 0.01; ***P < 0.005; t-test).
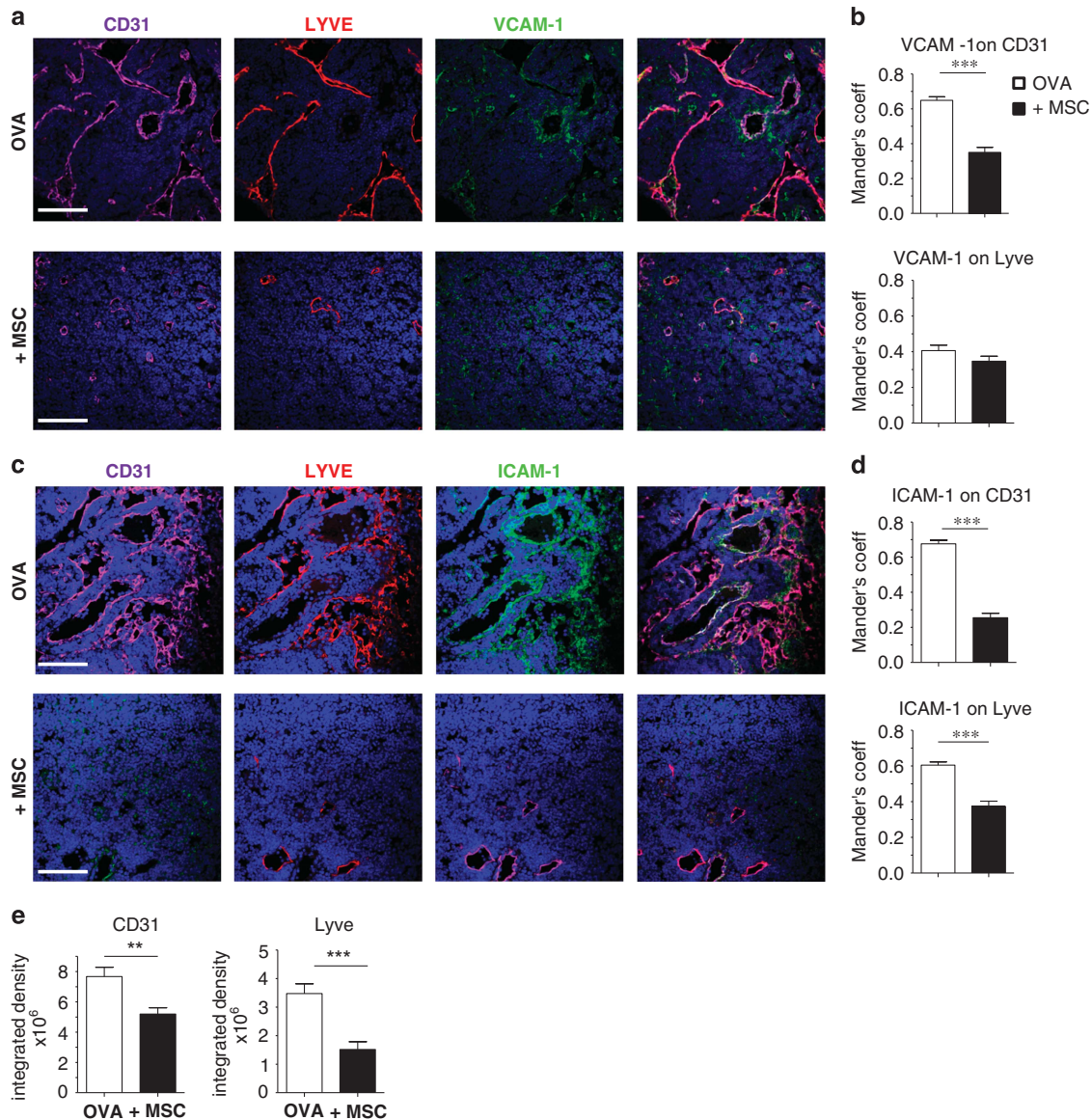
Figure 2. MSC inhibit endothelial activation in dLNs. Mice were treated as in Figure 1a and, on day 5, dLNs were collected, stained and analyzed by confocal microscopy. (**a**, **c**) 8-μm frozen section was stained with anti-CD31, anti-Lyve-1 and anti-VCAM-1 or anti-ICAM-1, as indicated (10×, scale bar 200 mm). (**b**, **d**) Mander's colocalization coefficient quantifies the degree of overlap. (**e**) Integrated density quantifies the CD31 and Lyve-1 immunopositivity amount on cross sections of lymph node. In all graphs, error bar represents s.e. (**$P < 0.01$, ***$P < 0.005$; t-test).

Analysis of entire LNs by optical projection tomography, which allows a three-dimensional reconstruction of the HEV network, allowed us to examine the morphologic alterations that occur in HEV expansion after immunization with CFA/OVA in the presence or absence of MSC. HEVs were labelled before imaging by intravenous injection of fluorophore-tagged MECA-79, which recognizes the PNAd epitope on the luminal surface (Figure 4a, Supplementary videos S3 and S4). The HEV length was significantly impaired in mice transplanted with MSC (Figure 4b) and the analysis of the HEV volume suggested a tendency toward vessel narrowing, although in this case the difference did not reach statistical significance (Figure 4c). In addition, the morphology of the HEV network was affected by MSC, as shown by the significant decrease in the number of branches and segments (Figures 4d and e), indicating that MSC limit both HEV elongation and arborization.

The previous observation prompted us to address whether MSC impair leukocyte homing to inflamed LNs. Fluorescently labelled naive T cells were injected i.v. in mice previously immunized with CFA/OVA, and transplanted or not with MSC. After 20 min, alexa633-conjugated MECA-79 and MEL-14 mAbs were i.v. injected to stain HEV and block L-selectin, respectively, and, after 20 additional minutes, the dLNs were harvested and prepared for two-photon microscopy acquisition (Figure 4f).[22] The analysis demonstrated that MSC transplantation inhibited T-cell homing into the inflamed LNs (Figure 4g).

Endothelial cells are a direct target of MSC

To understand whether the inhibition of endothelial cell activation and proliferation observed in immunized mice treated with MSC was due to a direct effect of MSC on endothelial cells, we analyzed the effects of MSC supernatants in various in vitro assays using a mouse vascular endothelial (1G11) and two mouse lymphatic endothelial (MELC and SVEC4-10) cell lines.[30–32] MSC were first expanded as an adherent monolayer until confluence, and were
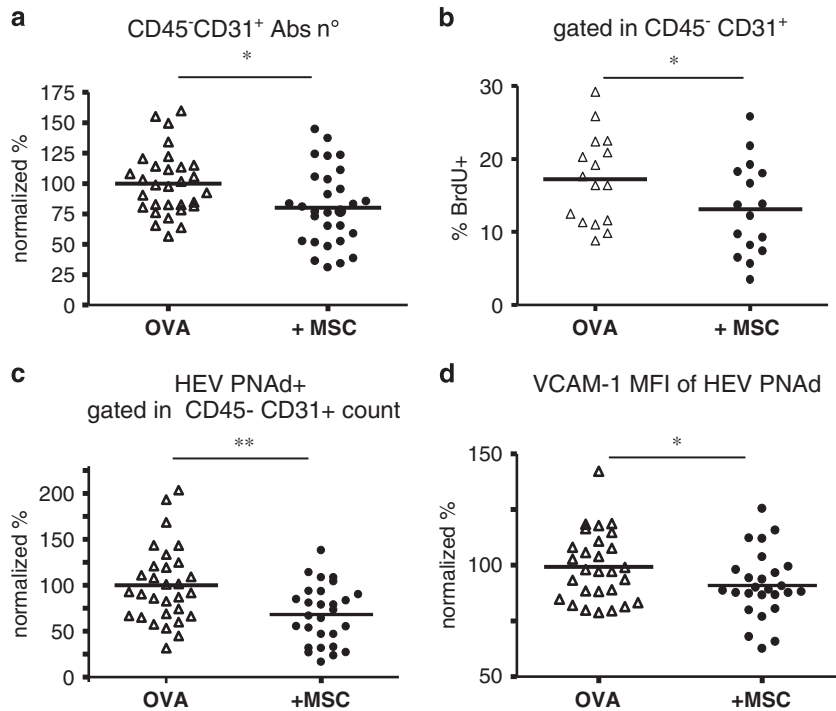
Figure 3. MSC inhibit HEV activation and proliferation in vivo. Mice were treated as illustrated in Figure 1a and dLNs were collected, digested and analyzed by flow cytometry. The graphs show (a) the absolute number of CD45⁻CD31⁺ cells per single LN expressed as normalized percentage on CFA/OVA (t-test), (b) BrdU incorporation cytometry after 48 h (Mann–Whitney test), (c) HEV cell numbers and (d) mean fluorescence intensity (MFI) of VCAM-1 expression on HEV (t-test) (*$P < 0.05$; **$P < 0.01$).

then stimulated for 24 h in the presence or absence of IL-1β, IL-6 and TNF-α to resemble the inflammatory milieu that MSC find in vivo.[33,34] MSC supernatant was collected as conditioned medium (CM) 18 h after cytokine withdrawal.

First, we analyzed the effect of MSC secretion on in vitro angiogenesis using the tube formation assay.[35] The soluble factors released by stimulated MSC strongly inhibited the ability of SVEC4-10 cells to form tube networks, whereas the medium collected from the unstimulated MSC (unst MSC-CM) had no effect (Figures 5a and b), indicating that in an inflammatory environment MSC can directly inhibit angiogenesis. This effect was also confirmed on another lymphatic endothelial cell line (MELC; Supplementary Figure S2). On the basis of these results and of the published literature,[33,34] in the following experiments we focused on the effects of the MSC-CM only.

As the in vivo data indicated that MSC transplantation affects the expression of adhesion molecules on endothelial cells (Figure 2b), we analyzed the expression of VCAM-1 and ICAM-1 on MELC and 1G11 cells treated with 20 ng/ml TNF-α for 24 h,[30,31] in the presence or in the absence of MSC-CM. In agreement with the previous data, the MSC-CM significantly reduced the expression of VCAM-1 and ICAM-1 on MELC (Figures 5c and e) and the expression of VCAM-1 on 1G11 cells (Figures 5d and f).

Expression of VCAM-1 and ICAM-1 on endothelial cells is regulated by NF-kB;[36] and thus, we examined the nuclear localization of NF-kB complexes using immunofluorescence microscopy. As expected, in both MELC and 1G11 cells TNF-α stimulation resulted in prompt translocation of p65 from the cytoplasm into the nucleus. MSC-CM inhibited NF-kB translocation in both cell lines (Figures 5g–j).

Altogether, these data indicate that endothelial cell activation is directly inhibited by soluble factors released by MSC exposed to inflammatory cytokines.

MSC inhibit in vitro angiogenesis through the release of TIMP-1

In an effort to understand the molecular mechanisms responsible for the observed effects of MSC, we performed shotgun proteomic characterization of the MSC secretome, comparing the supernatants collected from MSC stimulated (MSC-CM) or not (unst MSC-CM) with inflammatory cytokines. As detailed in Materials and methods, only proteins present and quantified in at least three out of five technical repeats, in both biological replicates, were considered as positively identified; 1613 and 1630 proteins were measured in the secretome of control and stimulated MSC, respectively.

Differential expression was considered as significant if (a) a protein was present only in MSC-CM or in control or (b) its LFQ intensity resulted statistically significant as calculated by Perseus (t-test cutoff at 1% permutation-based false discovery rate). According to this analysis, 7.6 or 8.3% of the proteins detected in the secretome of control or stimulated MSC, respectively, were differentially expressed, either upregulated or downregulated. These proteins were clustered according to their functions using the DAVID platform[37] filtered for significant Gene Ontology Biological Process (GOBP) terms using a P-value of < 0.05.

Concerning the 52 proteins that were significantly downregulated or present only in the secretome of unstimulated MSC (Supplementary Table S1), GO analysis revealed that most terms are related to metabolic processes (Supplementary Figure S3). As for the 89 proteins that were significantly upregulated or present only in the secretome of stimulated MSC (Supplementary Table S2 and Figure 6a), GO analysis indicated that 18 and 30% of the proteins belong to categories that are related to regulation of angiogenesis and inflammation processes, respectively (Supplementary Table S2 and Figure 6b). In particular, the presence of an 'angiogenesis-related' signature among upregulated proteins was also confirmed by preliminary analyses of
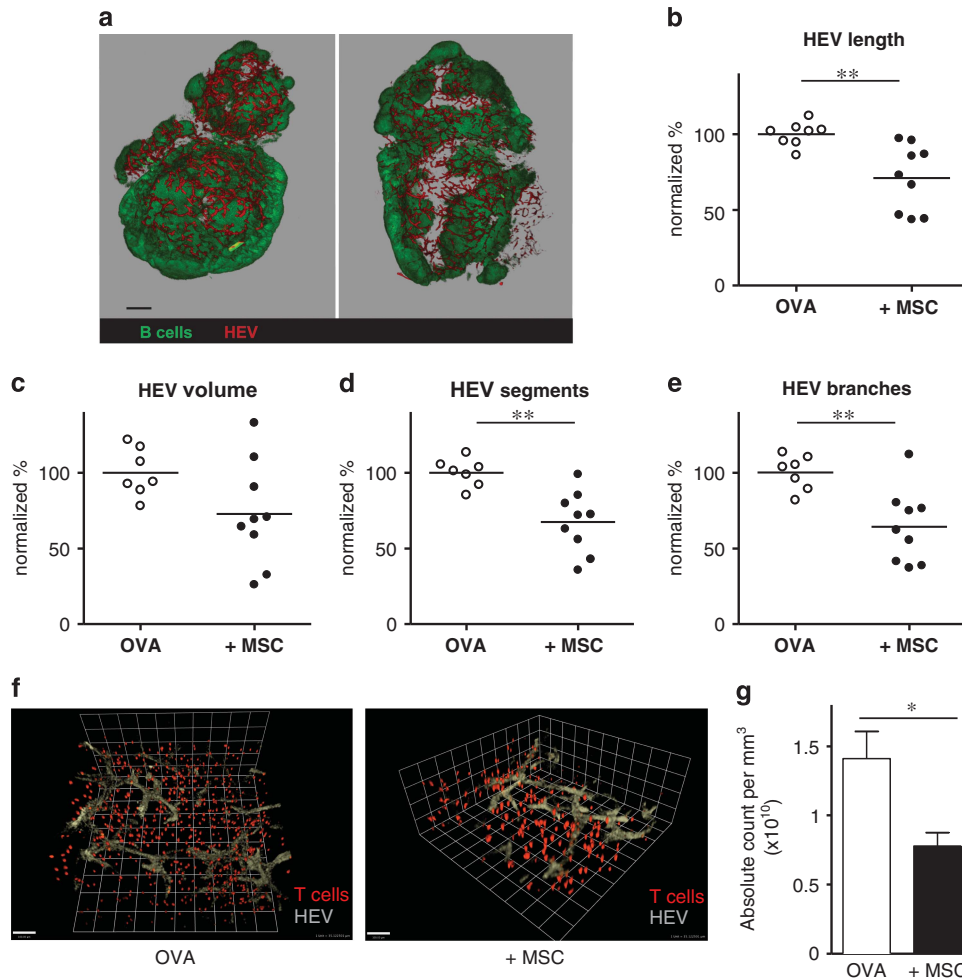
Figure 4. MSC suppress HEV lengthening and branching. (**a–e**) Mice were treated as described in Figure 1a, and on day 4 brachial LNs were prepared for OPT imaging (Meca-79 Alexa-594 and B220 Alexa-488). (**a**) Representative images from OPT scanning (scale bar, 400 μm). (**b**) Total HEV length per LN. (**c**) Total HEV volume per LN. (**d**) Number of HEV segments per LN. (**e**) Number of branch points per LN. (**f, g**) 3D immunofluorescence of lymphocyte homing in the presence of MSC tested at day 3 post immunization. (**f**) Representative images. (**g**) Absolute counts per mm^3 in OVA and OVA+MSC-treated mice, with error bars representing s.e. (*$P < 0.05$, **$P < 0.01$; t-test).

human MSC secretome, which reveals that all the 16 upregulated proteins in stimulated MSC secretome common to human and mouse are modulators of angiogenesis (Supplementary Table S3).

Among the several proteins upregulated in MSC by the inflammatory cytokines that have a direct or indirect effect on endothelial cells, we focused our attention on the TIMP-1 because of its well-known anti-angiogenic properties.[38] We thus used the tube formation assay to analyze the effect of MSC-derived TIMP-1 on angiogenesis. Although the blocking anti-TIMP-1 antibody had no effect on the ability of endothelial cells to form tubes when cultured in the supernatants of unstimulated MSC, it totally reverted the anti-angiogenic properties of the supernatant from stimulated MSC (Figure 7a), indicating that, al least in this *in vitro* setting, TIMP-1 is one of the key MSC-secreted molecules targeting the endothelium. In an *in vivo* setting, the injection of neutralizing anti-TIMP-1 antibody[19] 1 day after MSC transplantation reverted the MSC-induced reduction of endothelial cell numbers and HEV in dLNs (Figures 7b–d), suggesting that TIMP-1 may be directly responsible for the anti-inflammatory effects of MSC on LNs. To confirm this hypothesis, we used a siRNA approach to knock down TIMP-1 expression in MSC (Supplementary Figure S4). Again, the absolute cell numbers of endothelial cells and HEV in dLN were reduced by MSC transfected

with the scramble siRNA control but not by MSC with TIMP-1 siRNA (Figures 7e–g).

On the basis of these results, we speculated that overexpression of TIMP-1 might be sufficient to mimic the effects of MSC transplantation, in terms of inhibition of angiogenesis in the inflamed lymph nodes. TIMP-1 overexpression by AAV9-mediated gene transfer[20] in mice immunized with CFA/OVA (Figure 8a) inhibited the inflammatory reaction in the draining LNs, as indicated by the reduced total cellularity (Figure 8b), which was due to a decreased number of both CD45$^+$ cells (Figure 8c) and endothelial and HEV cells (Figures 8d and e).

DISCUSSION

MSC have been studied across a range of clinical indications and represent a promising therapeutic approach in many diseases in view of their potent immunomodulatory properties. To design better therapeutic protocols and define the clinical endpoints, it is important to identify the specific targets of MSC anti-inflammatory action *in vivo*. In this study, we have demonstrated that LN endothelial cells and HEV are a direct target of MSC-based therapy.

LNs are the organs where the initiation of immune responses takes place and their structure guides and organizes the crosstalk
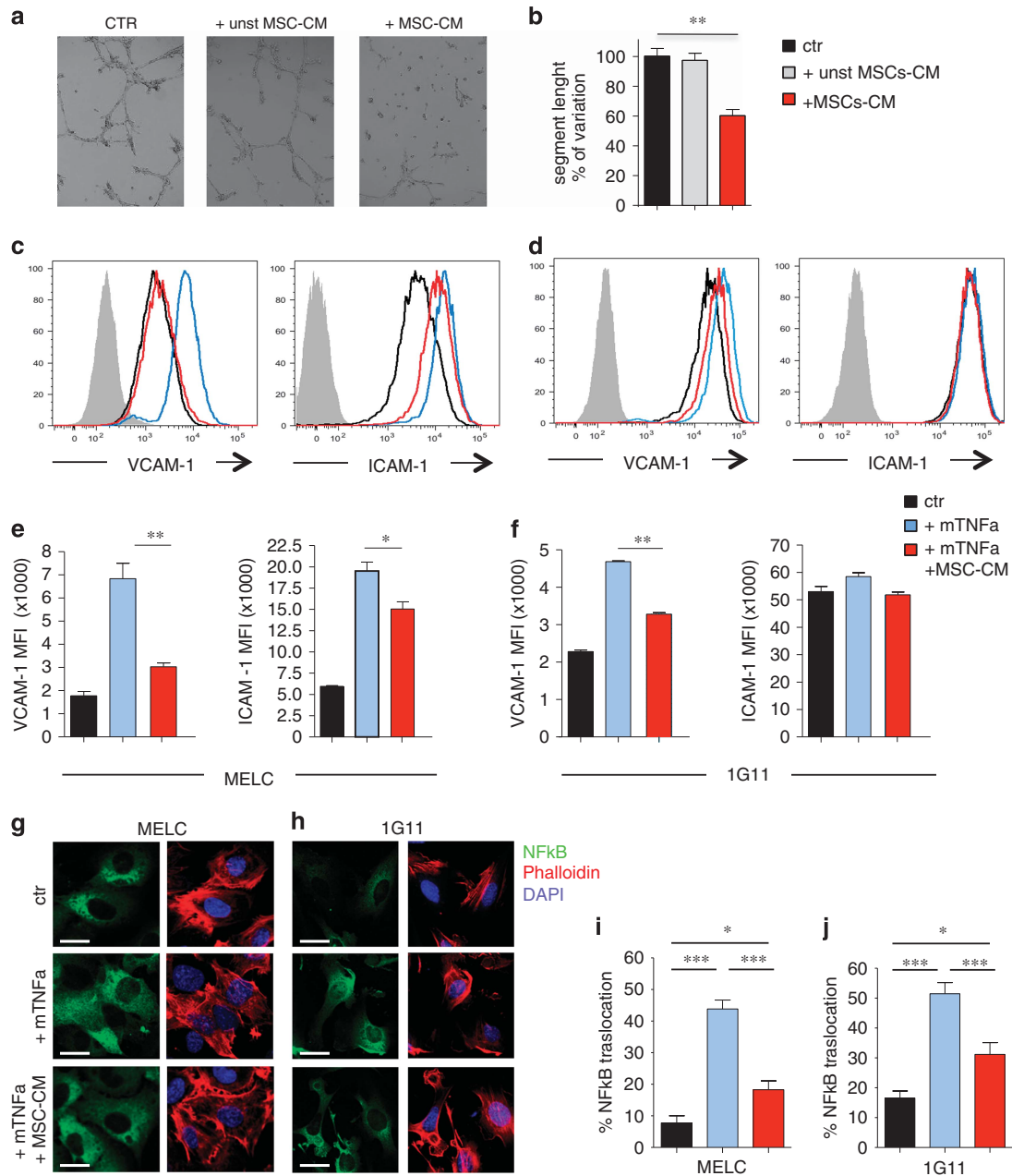
Figure 5. Endothelial cells are a direct target of MSC-secreted molecules. The supernatant of MSC stimulated with IL-1b, IL-6 and TNF-a (MSC-CM) or unstimulated MSC (unst MSC) was collected as described in Materials and methods, and its effect on endothelial cell lines activation was determined. (**a, b**) SVEC4-10 network formation. Representative images at 6 h and segment length quantification indicated as % of variation in comparison with control condition. Data are expressed as mean ± s.e.m. and represent the pool of three experiments (t-test). (**c, d**) Expression of endothelial adhesion molecules. Representative histograms showing the mean fluorescence intensity (MFI) of VCAM-1 and ICAM-1 on MELC and 1G11 endothelial cell line. (**e, f**) Quantitative analyses of (**c**) and (**d**), respectively (t-test). (**g–j**) TNF-a induced NF-kB translocation. Representative confocal images (×40) of MELC (**g**) or 1G11 (**h**) cells stained for NF-kB and phalloidin. Scale bar 10 um. (**I, j**) Quantification of NF-kB translocation into the nucleus expressed as percentage of the total (one representative experiment out of three; one-way ANOVA) (*$P < 0.05$; **$P < 0.01$; ***$P < 0.0001$).

between lymphocytes and antigen-presenting cells during both normal responses to pathogens and immune-mediated diseases, such as autoimmunity, allergy or graft-versus-host disease.[39] When a robust immune response develops, infiltrating and dividing lymphocytes markedly increase LNs cellularity, leading to organ expansion. During this swelling, there is massive endothelial cell proliferation and vascular expansion occurs.[40] Both acute and chronic inflammatory processes are indeed associated with pronounced vascular remodelling. Angiogenesis and lymph angiogenesis, the growth of new blood vessels and

lymphatic vessels from pre-existing ones, are involved in a number of physiological and pathological conditions, such as wound healing, tumor growth, rheumatoid arthritis, inflammatory bowel disease and asthma.[41] Thus, the identification of therapies that specifically inhibit angiogenesis may represent a weapon to reduce inflammation and prevent disease progression.[16]

Recently, it was demonstrated that MSC have a potent stabilizing effect on the vascular endothelium, having the capacity of inhibiting endothelial permeability after traumatic brain injury[42] and in hemorrhagic shock.[43] Our results demonstrate that, during
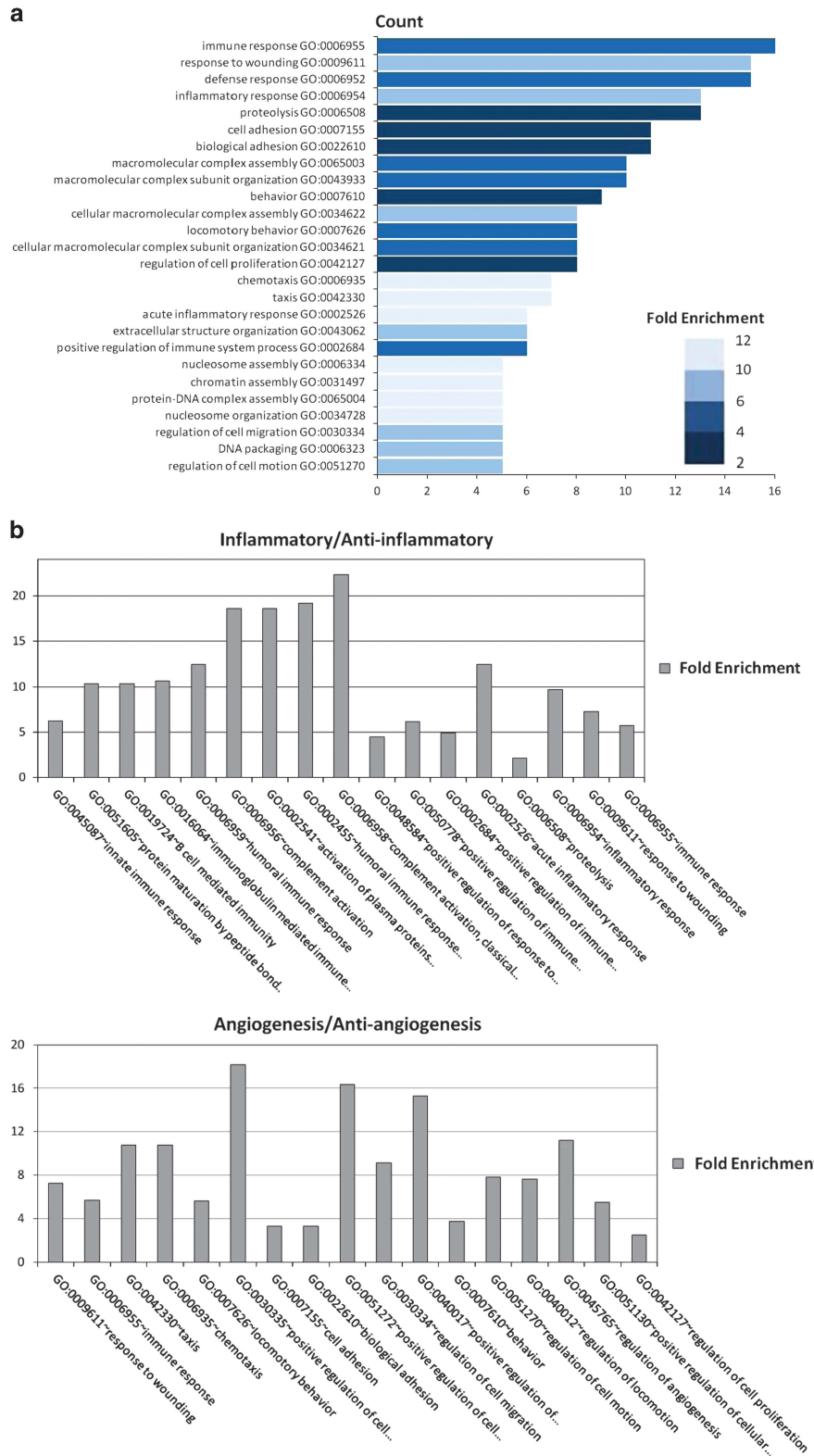
Figure 6. Distribution into biological processes of the proteins upregulated in MSC-CM. The proteins that were significantly upregulated or present only in MSC-CM were classified into different biological processes according to the GO classification system. (**a**) The bar chart shows the count of the top 26 most-enriched GO terms in MSC-CM versus unstimulated MSC-CM. Color coding indicates the fold enrichment. (**b**) Proteins categorized as modulators involved in inflammation processes and/or angiogenesis. The histograms report the GOBP groups related to angiogenesis or inflammation.
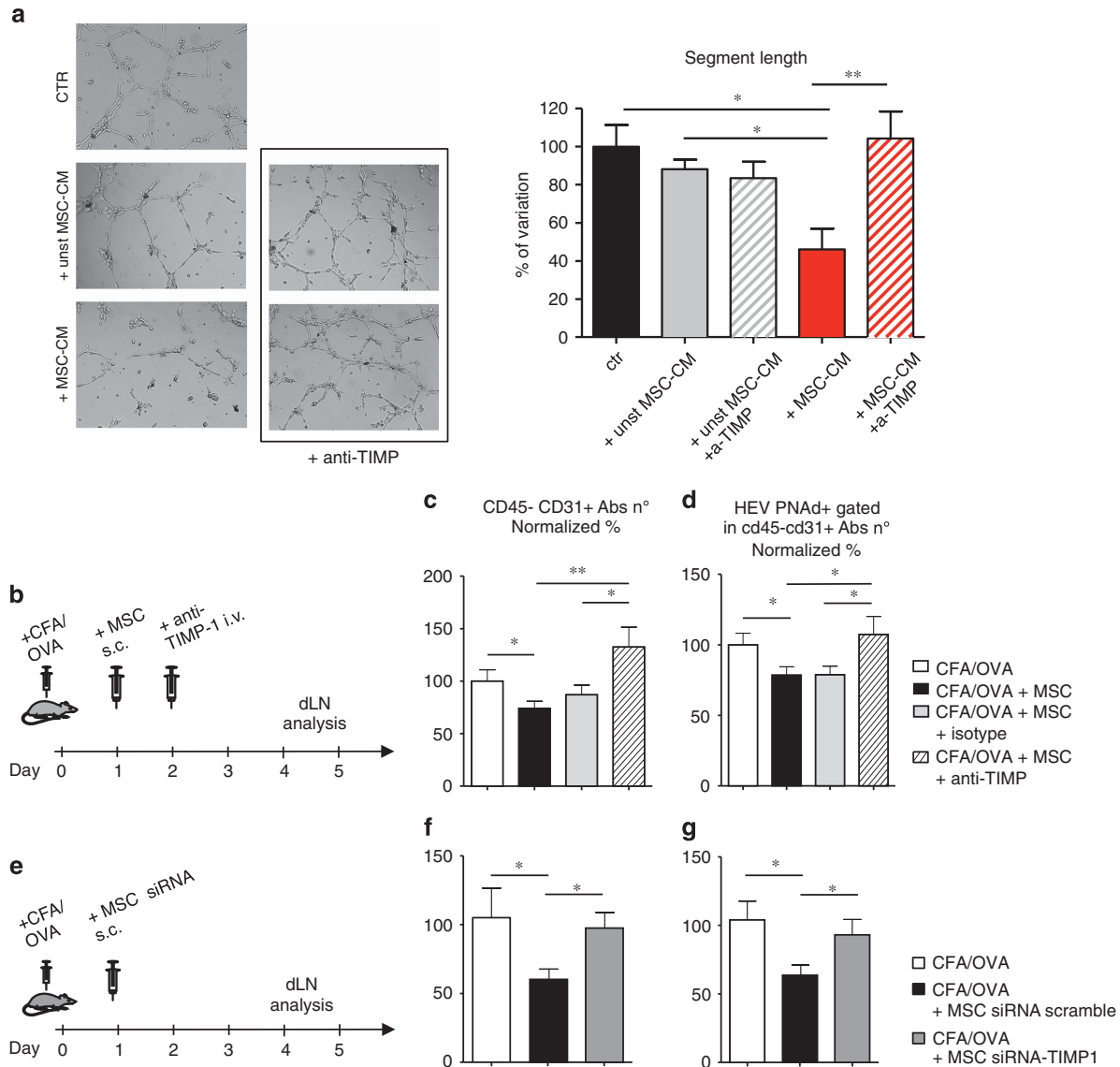
Figure 7. TIMP-1 mediates the anti-angiogenic effect of MSC-CM *in vitro* and the anti-inflammatory effect of MSC *in vivo*. SVEC4-10 network formation in matrigel in the presence of MSC-CM or unst MSC-CM and anti-TIMP-1 blocking antibody. (**a**) anti-mTIMP1 blocking antibody restores SVEC4-10 network formation in matrigel in the presence of MSC-CM. Representative images at 6 h (left) and segment length quantification as percentage of variation (right) are shown. Data are expressed as mean ± s.e.m. (*$P < 0.05$, **$P < 0.01$; one-way ANOVA). (**b**) Diagram of the experimental protocol designed to block the TIMP-1 activity during the anti-inflammatory effects of MSC. Mice were immunized in the dorsal region with CFA/OVA on day 0 and, on day 1, three groups of animals received subcutaneous injection of 10^6 MSC in the lumbar region. Eighteen hours after MSC transplantation, goat polyclonal anti-TIMP-1 IgG or isotype-matched goat IgG was i.v. administrated. On day 4,*-3 brachial LNs were collected, processed and analyzed by flow cytometry; (**c, d**) the graphs show the absolute number of CD45⁻CD31⁺ cells and HEV PNAd⁺ cells per single LN, expressed as normalized percentage on CFA/OVA (*t*-test). (**e**) Diagram of the experimental protocol designed to investigate the contribution of MSC-derived TIMP-1 on dLN endothelium. Mice were immunized in the dorsal region with CFA/OVA on day 0. The day after, two groups of animals received in the lumbar region subcutaneous injection of 10^6 MSC transfected with either scramble control siRNA or siRNA specific for TIMP-1, respectively. On day 4, brachial LNs were collected, processed and analyzed by flow cytometry; (**f, g**) graphs showing the absolute number of CD45⁻CD31⁺ cells and HEV PNAd⁺ cells per single dLN. Data are expressed as normalized percentage on CFA/OVA (Mann–Whitney test) (*$P < 0.05$; **$P < 0.01$).

an immune response, MSC inhibit HEV proliferation, activation and elongation in dLNs, thus reducing the recruitment of immune cells. In agreement with our data, homing of dendritic cell to dLNs was reduced in the presence of MSC in several mouse models[44,45] and *in vitro* co-cultures of MSC with endothelial cells down-regulated cytokine-induced recruitment of neutrophils and lymphocytes.[46]

In our study, the effects of MSC on endothelial cell activation, HEV elongation and T-cell trafficking do not require MSC homing to LNs and are all mediated by soluble factors released by MSC.

This is in agreement with another study showing an anti-angiogenic activity for soluble factors present in media derived from MSC/glioma co-cultures.[47] The proteomic analysis of the MSC secretome indicated that, upon activation by inflammatory cytokines, MSC upregulate the expression of several proteins potentially affecting angiogenesis and inflammation through multiple pathways. Interestingly, when we compared the secretomes of human and mouse MSC, we found that only 16 proteins are upregulated in both cell types and 11 of them modulate angiogenesis directly or indirectly, thus supporting the idea that
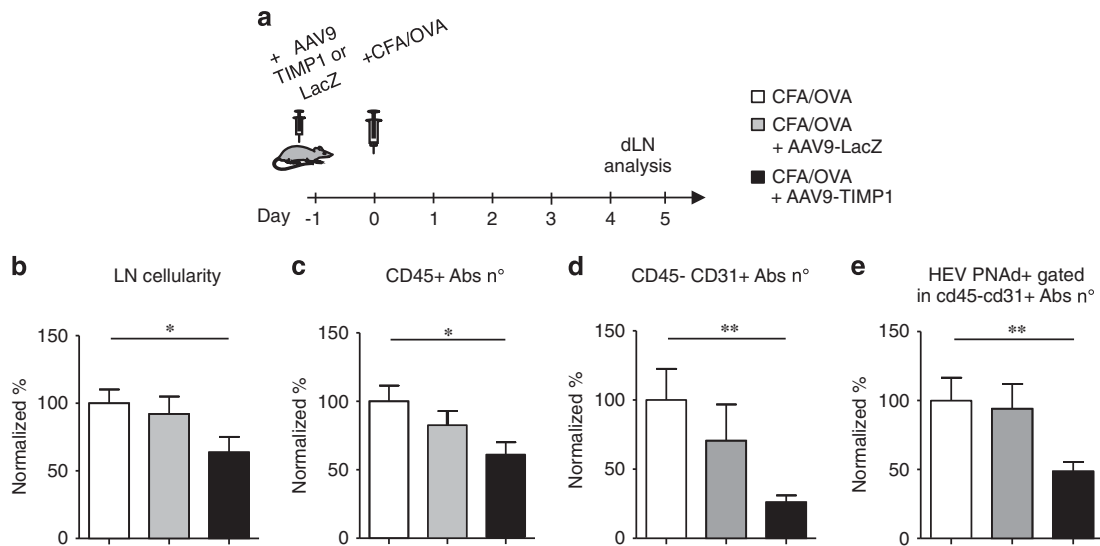
Figure 8. TIMP-1 overexpression *in vivo* mimics MSC transplantation. (**a**) Diagram of the experimental protocol designed to overexpress TIMP-1 in immunized mice. One day after AAV9-TIMP-1 or AAV9-LacZ administration (day 0), mice were immunized with CFA/OVA. Brachial dLNs were collected 4 days after immunization and processed for flow cytometry. The graphs show the absolute number of total cells (**b**), CD45$^+$ cells (**c**), CD45$^-$CD31$^+$ (**d**) and HEV PNAd$^+$ (**e**) cells per single LN, expressed as normalized percentage on CFA/OVA. Error bars represent standard error (*$P < 0.05$; **$P < 0.01$; Mann–Whitney test).

the endothelium is a specific target of MSC during inflammation. Notably, although many soluble factors released by cytokine-triggered MSC are positive regulators of angiogenesis, in the experimental system here described the overall *in vivo* effect of MSC is a reduced dLN vascular expansion.

Angiogenesis requires degradation of the vascular basement membrane and remodelling of the extracellular matrix to allow endothelial cells migration and invasion into the surrounding tissue. This process requires the action of matrix metalloproteinases (MMPs) that degrade both matrix and non-matrix proteins and have central roles in morphogenesis, wound healing, tissue repair and in progression of chronic diseases.[48] The balance between MMPs and their natural inhibitors, the TIMPs, is critical for extracellular matrix remodelling and angiogenesis. The TIMP family comprises four protease inhibitors: TIMP-1, TIMP-2, TIMP-3 and TIMP-4. With the exception of TIMP-4,[49] all three TIMPs inhibit angiogenesis *in vivo*,[38] although through diverse mechanisms. MSC secrete both MMPs and their inhibitors, and thus contribute to the regulation and protection of the perivascular niche.[50]

Using both *in vitro* and *in vivo* assays, we identified the metalloproteinase inhibitor TIMP-1 as the molecule responsible for the anti-angiogenic effects of MSC. TIMP-1 is known to inhibit endothelial cells migration by MMP-dependent and MMP-independent mechanisms.[51–53] The latter involve regulation of various biological processes such as cell growth, apoptosis and differentiation through the CD63 receptor.[54,55] In addition, TIMP-1 was shown to induce secretion of soluble VEGFR-1 by human endothelial cells, leading to a decrease of bioavailable VEGF and of blood vessel growth.[56] TIMP-3 has also been identified as a soluble factor produced by MSC with beneficial effects on endothelial cell function in a mouse model of traumatic brain injury;[57] however, we did not find evidence for TIMP-3 upregulation in the mouse or human MSC secretomes. It is likely that, *in vivo*, other soluble factors in addition to TIMP-1 contribute to MSC-mediated immune regulation: MSC are also known to produce prostaglandin E2 and thus inhibit the activation of macrophages,[58] which are a source of multiple growth factors that enhance endothelial cell proliferation and survival.[59] Indeed, we confirmed prostaglandin E2 secretion by stimulated MSC (not shown) and, in addition, we found that

MSC release several other anti-inflammatory lipids, such as resolvinD1 and LipoxinA4 (not shown) that may also affect endothelial cell activation and/or proliferation. Another interesting mediator found in the MSC secretome is the soluble form of VCAM-1 (sVCAM-1). High levels of sVCAM-1 have been detected in the synovial fluid of patients with rheumatoid arthritis[60] and in the blood of patients with different types of cancers,[61] but its origin is not entirely clear and our data suggest that MSC may represent an important source of this molecule. Although sVCAM-1 is described as a promoter of angiogenesis,[62] by altering leukocyte trafficking[63] or inhibiting T-cell activation,[64] it may contribute to the MSC-induced suppression of T-cell recruitment that we observed in this study.

The results presented here clearly position endothelial cells as a key target of MSC-mediated immunomodulation during ongoing inflammatory responses and pave the way for developing strategies that exploit MSC-mediated inhibition of lymph-node angiogenesis in the treatment of inflammation-associated pathologies. Furthermore, by identifying TIMP-1 as a critical effector of the anti-inflammatory properties of MSC, this study pinpoints a potential new biomarker in clinical settings. Further studies on the role of TIMP-1 in human MSC are required to confirm its correlation with clinical outcomes or its value in selecting the best source of MSC for immunomodulation.

CONFLICT OF INTEREST

The authors declare no conflict of interest.

REFERENCES

1 Caplan AI. Mesenchymal stem cells. *J Orthop Res* 1991; **9**: 641–650.

2 Crisan M, Yap S, Casteilla L, Chen CW, Corselli M, Park TS *et al.* A perivascular origin for mesenchymal stem cells in multiple human organs. *Cell Stem Cell* 2008; **3**: 301–313.

3 Covas DT, Panepucci RA, Fontes AM, Silva Jr WA, Orellana MD, Freitas MC *et al.* Multipotent mesenchymal stromal cells obtained from diverse human tissues share functional properties and gene-expression profile with CD146+ perivascular cells and fibroblasts. *Exp Hematol* 2008; **36**: 642–654.

4 Hellstrom M, Gerhardt H, Kalen M, Li X, Eriksson U, Wolburg H *et al.* Lack of pericytes leads to endothelial hyperplasia and abnormal vascular morphogenesis. *J Cell Biol* 2001; **153**: 543–553.

5 Frenette PS, Pinho S, Lucas D, Scheiermann C. Mesenchymal stem cell: keystone of the hematopoietic stem cell niche and a stepping-stone for regenerative medicine. *Annu Rev Immunol* 2013; **31**: 285–316.

6 Sensebe L, Krampera M, Schrezenmeier H, Bourin P, Giordano R. Mesenchymal stem cells for clinical application. *Vox Sang* 2010; **98**: 93–107.

7 Zappia E, Casazza S, Pedemonte E, Benvenuto F, Bonanni I, Gerdoni E *et al.* Mesenchymal stem cells ameliorate experimental autoimmune encephalomyelitis inducing T-cell anergy. *Blood* 2005; **106**: 1755–1761.

8 Djouad F, Fritz V, Apparailly F, Louis-Plence P, Bony C, Sany J *et al.* Reversal of the immunosuppressive properties of mesenchymal stem cells by tumor necrosis factor alpha in collagen-induced arthritis. *Arthritis Rheum* 2005; **52**: 1595–1603.

9 Zanotti L, Sarukhan A, Dander E, Castor M, Cibella J, Soldani C *et al.* Encapsulated mesenchymal stem cells for in vivo immunomodulation. *Leukemia* 2013; **27**: 500–503.

10 Murphy MB, Moncivais K, Caplan AI. Mesenchymal stem cells: environmentally responsive therapeutics for regenerative medicine. *Exp Mol Med* 2013; **45**: e54.

11 Sala E, Genua M, Petti L, Anselmo A, Arena V, Cibella J *et al.* Mesenchymal stem cells reduce colitis in mice via release of TSG6, independently of their localization to the intestine. *Gastroenterology* 2015; **149**: 163–176 e20.

12 Strieter RM, Burdick MD, Gomperts BN, Belperio JA, Keane MP. CXC chemokines in angiogenesis. *Cytokine Growth Factor Rev* 2005; **16**: 593–609.

13 Charo IF, Ransohoff RM. The many roles of chemokines and chemokine receptors in inflammation. *N Engl J Med* 2006; **354**: 610–621.

14 De Bruyn PP, Cho Y. Structure and function of high endothelial postcapillary venules in lymphocyte circulation. *Curr Top Pathol* 1990; **84**: 85–101.

15 Forster R, Schubel A, Breitfeld D, Kremmer E, Renner-Muller I, Wolf E *et al.* CCR7 coordinates the primary immune response by establishing functional micro-environments in secondary lymphoid organs. *Cell* 1999; **99**: 23–33.

16 Pober JS, Sessa WC. Evolving functions of endothelial cells in inflammation. *Nat Rev Immunol* 2007; **7**: 803–815.

17 Phillips RJ, Mestas J, Gharaee-Kermani M, Burdick MD, Sica A, Belperio JA *et al.* Epidermal growth factor and hypoxia-induced expression of CXC chemokine receptor 4 on non-small cell lung cancer cells is regulated by the phosphatidy-linositol 3-kinase/PTEN/AKT/mammalian target of rapamycin signaling pathway and activation of hypoxia inducible factor-1alpha. *J Biol Chem* 2005; **280**: 22473–22481.

18 Medzhitov R. Origin and physiological roles of inflammation. *Nature* 2008; **454**: 428–435.

19 Crocker SJ, Frausto RF, Whitmire JK, Benning N, Milner R, Whitton JL. Amelioration of coxsackievirus B3-mediated myocarditis by inhibition of tissue inhibitors of matrix metalloproteinase-1. *Am J Pathol* 2007; **171**: 1762–1773.

20 Zacchigna S, Pattarini L, Zentilin L, Moimas S, Carrer A, Sinigaglia M *et al.* Bone marrow cells recruited through the neuropilin-1 receptor promote arterial formation at the sites of adult neoangiogenesis in mice. *J Clin Invest* 2008; **118**: 2062–2075.

21 Kumar V, Scandella E, Danuser R, Onder L, Nitschke M, Fukui Y *et al.* Global lymphoid tissue remodeling during a viral infection is orchestrated by a B cell-lymphotoxin-dependent pathway. *Blood* 2010; **115**: 4725–4733.

22 Boscacci RT, Pfeiffer F, Gollmer K, Sevilla AI, Martin AM, Soriano SF *et al.* Comprehensive analysis of lymph node stroma-expressed Ig superfamily members reveals redundant and nonredundant roles for ICAM-1, ICAM-2, and VCAM-1 in lymphocyte homing. *Blood* 2010; **116**: 915–925.

23 Roy D, Steyer GJ, Gargesha M, Stone ME, Wilson DL. 3D cryo-imaging: a very high-resolution view of the whole mouse. *Anat Rec (Hoboken)* 2009; **292**: 342–351.

24 Roy D, Gargesha M, Steyer GJ, Hakimi P, Hanson RW, Wilson DL. Multi-scale characterization of the PEPCK-C mouse through 3D cryo-imaging. *Int J Biomed Imaging* 2010; **2010**: 105984.

25 Schrepfer S, Deuse T, Lange C, Katzenberg R, Reichenspurner H, Robbins RC *et al.* Simplified protocol to isolate, purify, and culture expand mesenchymal stem cells. *Stem Cells Dev* 2007; **16**: 105–107.

26 Schrepfer S, Deuse T, Reichenspurner H, Fischbein MP, Robbins RC, Pelletier MP. Stem cell transplantation: the lung barrier. *Transplant Proc* 2007; **39**: 573–576.

27 Lee RH, Pulin AA, Seo MJ, Kota DJ, Ylostalo J, Larson BL *et al.* Intravenous hMSCs improve myocardial infarction in mice because cells embolized in lung are activated to secrete the anti-inflammatory protein TSG-6. *Cell Stem Cell* 2009; **5**: 54–63.

28 Gargesha M, Qutaish MQ, Roy D, Steyer GJ, Watanabe M, Wilson DL. Visualization of color anatomy and molecular fluorescence in whole-mouse cryo-imaging. *Comput Med Imaging Graph* 2011; **35**: 195–205.

29 Kumar V, Chyou S, Stein JV, Lu TT. Optical projection tomography reveals dynamics of HEV growth after immunization with protein plus CFA and features shared with HEVs in acute autoinflammatory lymphadenopathy. *Front Immunol* 2012; **3**: 282.

30 Sironi M, Conti A, Bernasconi S, Fra AM, Pasqualini F, Nebuloni M *et al.* Generation and characterization of a mouse lymphatic endothelial cell line. *Cell Tissue Res* 2006; **325**: 91–100.

31 Dong QG, Bernasconi S, Lostaglio S, De Calmanovici RW, Martin-Padura I, Breviario F *et al.* A general strategy for isolation of endothelial cells from murine tissues. Characterization of two endothelial cell lines from the murine lung and subcutaneous sponge implants. *Arterioscler Thromb Vasc Biol* 1997; **17**: 1599–1604.

32 O'Connell KA, Edidin M. A mouse lymphoid endothelial cell line immortalized by simian virus 40 binds lymphocytes and retains functional characteristics of normal endothelial cells. *J Immunol* 1990; **144**: 521–525.

33 Bernardo ME, Fibbe WE. Mesenchymal stromal cells: sensors and switchers of inflammation. *Cell Stem Cell* 2013; **13**: 392–402.

34 Groh ME, Maitra B, Szekely E, Koc ON. Human mesenchymal stem cells require monocyte-mediated activation to suppress alloreactive T cells. *Exp Hematol* 2005; **33**: 928–934.

35 Arnaoutova I, Kleinman HK. In vitro angiogenesis: endothelial cell tube formation on gelled basement membrane extract. *Nat Protoc* 2010; **5**: 628–635.

36 Zhou Z, Connell MC, MacEwan DJ. TNFR1-induced NF-kappaB, but not ERK, p38MAPK or JNK activation, mediates TNF-induced ICAM-1 and VCAM-1 expression on endothelial cells. *Cell Signal* 2007; **19**: 1238–1248.

37 Huang, da W, Sherman BT, Lempicki RA. Systematic and integrative analysis of large gene lists using DAVID bioinformatics resources. *Nat Protoc* 2009; **4**: 44–57.

38 Lambert E, Dasse E, Haye B, Petitfrere E. TIMPs as multifacial proteins. *Crit Rev Oncol Hematol* 2004; **49**: 187–198.

39 Lin KL, Fulton LM, Berginski M, West ML, Taylor NA, Moran TP *et al.* Intravital imaging of donor allogeneic effector and regulatory T cells with host dendritic cells during GVHD. *Blood* 2014; **123**: 1604–1614.

40 Webster B, Ekland EH, Agle LM, Chyou S, Ruggieri R, Lu TT. Regulation of lymph node vascular growth by dendritic cells. *J Exp Med* 2006; **203**: 1903–1913.

41 Zgraggen S, Ochsenbein AM, Detmar M. An important role of blood and lymphatic vessels in inflammation and allergy. *J Allergy* 2013; **2013**: 672381.

42 Pati S, Khakoo AY, Zhao J, Jimenez F, Gerber MH, Harting M *et al.* Human mesenchymal stem cells inhibit vascular permeability by modulating vascular endothelial cadherin/beta-catenin signaling. *Stem Cells Dev* 2011; **20**: 89–101.

43 Pati S, Gerber MH, Menge TD, Wataha KA, Zhao Y, Baumgartner JA *et al.* Bone marrow derived mesenchymal stem cells inhibit inflammation and preserve vascular endothelial integrity in the lungs after hemorrhagic shock. *PLoS One* 2011; **6**: e25171.

44 Chiesa S, Morbelli S, Morando S, Massollo M, Marini C, Bertoni *et al.* Mesenchymal stem cells impair in vivo T-cell priming by dendritic cells. *Proc Natl Acad Sci USA* 2011; **108**: 17384–17389.

45 Lee HJ, Ko JH, Ko AY, Kim MK, Wee WR, Oh JY. Intravenous infusion of mesenchymal stem/stromal cells decreased CCR7(+) antigen presenting cells in mice with corneal allotransplantation. *Curr Eye Res* 2014; **39**: 780–789.

46 Luu NT, McGettrick HM, Buckley CD, Newsome PN, Rainger GE, Frampton J *et al.* Crosstalk between mesenchymal stem cells and endothelial cells leads to downregulation of cytokine-induced leukocyte recruitment. *Stem Cells* 2013; **31**: 2690–2702.

47 Ho IA, Toh HC, Ng WH, Teo YL, Guo CM, Hui KM *et al.* Human bone marrow-derived mesenchymal stem cells suppress human glioma growth through inhibition of angiogenesis. *Stem Cells* 2013; **31**: 146–155.

48 Nagase H, Visse R, Murphy G. Structure and function of matrix metalloproteinases and TIMPs. *Cardiovasc Res* 2006; **69**: 562–573.

49 Fernandez CA, Moses MA. Modulation of angiogenesis by tissue inhibitor of metalloproteinase-4. *Biochem Biophys Res Commun* 2006; **345**: 523–529.

50 Lozito TP, Tuan RS. Mesenchymal stem cells inhibit both endogenous and exogenous MMPs via secreted TIMPs. *J Cell Physiol* 2011; **226**: 385–396.

51 Reed MJ, Koike T, Sadoun E, Sage EH, Puolakkainen P. Inhibition of TIMP1 enhances angiogenesis in vivo and cell migration in vitro. *Microvasc Res* 2003; **65**: 9–17.

52 Ikenaka Y, Yoshiji H, Kuriyama S, Yoshii J, Noguchi R, Tsujinoue H et al. Tissue inhibitor of metalloproteinases-1 (TIMP-1) inhibits tumor growth and angiogenesis in the TIMP-1 transgenic mouse model. *Int J Cancer* 2003; **105**: 340–346.

53 Akahane T, Akahane M, Shah A, Connor CM, Thorgeirsson UP. TIMP-1 inhibits microvascular endothelial cell migration by MMP-dependent and MMP-independent mechanisms. *Exp Cell Res* 2004; **301**: 158–167.

54 Jung KK, Liu XW, Chirco R, Fridman R, Kim HR. Identification of CD63 as a tissue inhibitor of metalloproteinase-1 interacting cell surface protein. *EMBO J* 2006; **25**: 3934–3942.

55 Stetler-Stevenson WG. Tissue inhibitors of metalloproteinases in cell signaling: metalloproteinase-independent biological activities. *Sci Signal* 2008; **1**, re6.

56 Bruegmann E, Gruemmer R, Neulen J, Motejlek K. Regulation of soluble vascular endothelial growth factor receptor 1 secretion from human endothelial cells by tissue inhibitor of metalloproteinase 1. *Mol Hum Reprod* 2009; **15**: 749–756.

57 Menge T, Gerber M, Wataha K, Reid W, Guha S, Cox CS Jr. et al. Human mesenchymal stem cells inhibit endothelial proliferation and angiogenesis via cell-cell contact through modulation of the VE-Cadherin/beta-catenin signaling pathway. *Stem Cells Dev* 2013; **22**: 148–157.

58 Nemeth K, Leelahavanichkul A, Yuen PS, Mayer B, Parmelee A, Doi K et al. Bone marrow stromal cells attenuate sepsis via prostaglandin E(2)-dependent reprogramming of host macrophages to increase their interleukin-10 production. *Nat Med* 2009; **15**: 42–49.

59 Baer C, Squadrito ML, Iruela-Arispe ML, De Palma M. Reciprocal interactions between endothelial cells and macrophages in angiogenic vascular niches. *Exp Cell Res* 2013; **319**: 1626–1634.

60 Wellicome SM, Kapahi P, Mason JC, Lebranchu Y, Yarwood H, Haskard DO. Detection of a circulating form of vascular cell adhesion molecule-1: raised levels in rheumatoid arthritis and systemic lupus erythematosus. *Clin Exp Immunol* 1993; **92**: 412–418.

61 Dymicka-Piekarska V, Guzinska-Ustymowicz K, Kuklinski A, Kemona H. Prognostic significance of adhesion molecules (sICAM-1, sVCAM-1) and VEGF in colorectal cancer patients. *Thromb Res* 2012; **129**: e47–e50.

62 Koch AE, Halloran MM, Haskell CJ, Shah MR, Polverini PJ. Angiogenesis mediated by soluble forms of E-selectin and vascular cell adhesion molecule-1. *Nature* 1995; **376**: 517–519.

63 Kitani A, Nakashima N, Izumihara T, Inagaki M, Baoui X, Yu S et al. Soluble VCAM-1 induces chemotaxis of Jurkat and synovial fluid T cells bearing high affinity very late antigen-4. *J Immunol* 1998; **161**: 4931–4938.

64 Kitani A, Nakashima N, Matsuda T, Xu B, Yu S, Nakamura T et al. T cells bound by vascular cell adhesion molecule-1/CD106 in synovial fluid in rheumatoid arthritis: inhibitory role of soluble vascular cell adhesion molecule-1 in T cell activation. *J Immunol* 1996; **156**: 2300–2308.

Supplementary Information accompanies this paper on the Leukemia website (http://www.nature.com/leu)